Pamukkale Üniversitesi Mühendislik Bilimleri Dergisi

Pamukkale University Journal of Engineering Sciences

High efficiency design approach of a LLC resonant converter for on-board electrical vehicle battery charge applications

Elektrikli araç yerleşik batarya şarj uygulamaları için yüksek verimli bir LLC rezonanslı DC-DC dönüştürücünün tasarım yaklaşımı

Sevilay ÇETİN[1]*

[1]Technology Faculty, Pamukkale University, Denizli, Turkey.
scetin@pau.edu.tr

Abstract

In this study, an optimal design procedure of inductor-inductor-capacitor (LLC) resonant converter for on-board electrical vehicle (EV) battery charge applications based on high efficiency is proposed. In the design procedure, lithium-ion battery cells are used due to their high power density, higher voltage and current rates compared to a lead-acid battery cells. Thus, LLC resonant converter should be regulated the output voltage in a wide voltage range with different load conditions according to typical charging profile of lithium-ion battery. For the design procedure, basic operation characteristics of LLC resonant converter is defined and operation regions are discussed in terms of high efficiency. The operation regions of LLC resonant converter are discussed to regulate wide output voltage range. In order to reach high efficiency optimal design, efficiency calculations based on Saber simulation are extracted for discussed operation regions. The best efficiency values are obtained for the operation of above-below resonance. Finally, soft switching operation of the LLC resonant converter is validated by Saber simulation for wide output voltage range and with changing load current.

Keywords: Electrical vehicle battery charge, LLC resonant converter, High efficiency, Optimum design

Öz

Bu çalışmada, elektrikli araç (EV) yerleşik batarya şarj uygulamaları için indüktör-indüktör-kapasitor (LLC) rezonanslı bir dönüştürücünün yüksek verime dayalı optimum tasarım metodu sunulmuştur. Tasarım metodunda, lead-acid batarya hücreleri ile kıyaslandığında, yüksek güç yoğunluğu, yüksek akım ve gerilim değerlerine sahip olmaları gibi avantajları doğrultusunda lithium-ion batarya hücreleri kullanılmıştır. Böylece, LLC rezonanslı dönüştürücü, lithium-ion batarya şarj karakteristiğine göre geniş bir çıkış gerilimi aralığını farklı yük değerleri için regüle edebilmelidir. Tasarım yönteminde, LLC rezonanslı dönüştürücünün temel çalışma prensibi tanımlanmıştır ve çalışma bölgeleri yüksek verim açısından tartışılmıştır. LLC rezonanslı dönüştürücü, geniş bir aralıkta çıkış geriliminin regülasyonunu sağlayabilmesi için çalışma bölgeleri incelenmiştir. Yüksek verimli optimum tasarım yaklaşımına ulaşmak için çalışma durumlarına ait verim hesaplamaları Saber simülasyonu yardımı ile çıkarılmıştır. En iyi verim değerleri, rezonans frekansının hem altı hem üstü çalışma durumu için belirlenmiştir. Son olarak tasarlanan LLC rezonanslı dönüştürücünün yumuşak anahtarlamalı çalışması geniş bir gerilim ve yük aralığı için Saber simülasyonu ile doğrulanmıştır.

Anahtar kelimeler: Elektrikli araç batarya şarjı, LLC rezonanslı dönüştürücü, Yüksek verim, Optimum tasarım

1 Introduction

Recently, in the automotive industry, interest in electrical vehicle (EV) and plug-in hybrid EV technology increases greatly due to the depletion fossil fuels, global warming and the advantages in the economic area. On-board battery charging designs allow the user a flexibility to be charged EV's battery from any available power point. Thus, user interest in EV can be increased with reducing of battery charge depletion anxiety [1]. However, adapting battery charge module on board increases the volume, weight and cost of the EVs [2]-[4]. Therefore, in order to reduce volume and cost of the EVs, high power density and high efficiency battery chargers should be designed [5]-[7].

Lithium-ion batteries are usually preferred in EV battery charge system since their high power density, high voltage and current rate characteristics which are required for high power ratings [2],[8],[9]. The voltage range of a single lithium-ion battery cell is larger than lead-acid battery cell. Therefore, lithium-ion battery chargers should be designed to be regulated output voltage in a wide output voltage range.

A battery charger includes two stage: first stage is converters ac grid voltage to dc voltage with power factor correction function and the second stage used to regulate the output

voltage of battery charger with a followed dc-dc converter [1], [2],[10]-[12]. For the first stage, the conventional front-end PFC boost converter is usually used. For the second stage, in order to reach high power density and high efficiency, soft switching dc-dc converters allowing operation at high switching frequency are used. The phase shifted full bridge pulse width modulated converter and resonant converters are usually preferred [1],[10]-[13]. The soft switching operation of phase shifted full bridge converter becomes poor under light load conditions [14],[15]. However, battery charger works mostly under light load or no load conditions when battery is completely charged. The soft switching operation of resonant converters is maintained for very wide load ranges. In the resonant converters, output voltage regulation can be achieved by the change of the switching frequency and this is well known disadvantages of resonant converters. Among the resonant converters, LLC resonant converter is most preferred converter topology since it can be regulated the output voltage with a narrow switching frequency range [16].

The design procedure of LLC resonant converter for constant output voltage is discussed in many study in the literature for telecom or data center applications [17]-[20]. However, design approach for very wide output voltage range required for lithium-ion battery chargers is very different. Recently, some

studies have been presented related optimal design of LLC resonant converter for battery charge applications [10]-[13]. In [10], proposed design approach built based on lead-acid battery charge characteristic. The resonant tank parameters are determined based on battery charge characteristic and short-circuit condition of the resonant tank. In [11], a design procedure is proposed based on lead-acid battery charge characteristic and FHA. The parameter K (the ratio of the transformer magnetizing inductor L_m to the resonant inductor L_r) is determined according to two different charging points of lead-acid battery charge characteristic. Another design methodology of LLC converter is discussed in [12] based on lithium-ion battery charge characteristic. In the method, design constraints are extracted based on first harmonic approximation (FHA) and battery charge profile. The soft switching operation is analyzed for different operation region. In [13], the proposed method evaluates the time-weighted average efficiency of LLC converter based on lithium-ion battery charge characteristic. The optimal operation point to reach high efficiency is determined according to time-weighted of battery charge profile. In [21] and [22], proposed design approach is built based on FHA which is not reliable when switching frequency is far away from resonance frequency.

The proposed design techniques mentioned above gives good results. However, they don't include operation region optimization for lithium-ion battery charger regulating wide output voltage range. Therefore, this study evaluates the design approach of LLC resonant converter, giving best operation region, to reach high efficiency in lithium-ion EV battery chargers. The optimization is performed based on Saber simulation since the FHA is not reliable when switching frequency is far away from the resonance frequency. The optimization region is validated by simulation in terms of soft switching operation of the semiconductors and the output voltage regulation.

2 The basic principle of LLC resonant converter

A full bridge LLC resonant converter configuration is shown in Figure 1. In EV chargers, the full bridge configuration is usually used to provide high power requirements and to response fast charge demand. The resonant tank includes three components: the resonant inductor, L_r, the magnetizing inductance of the transformer, L_m, and the resonant capacitor, C_r. S1-S2 and S3-S4 are the MOSFET pairs applying square wave input voltage to the resonant tank. Each pair is turned-on and turned-off with 50% duty cycle in one switching period to produce symmetrical square wave voltage across the resonant tank. A center-tapped rectifier is used for the secondary side of LLC converter. DR1-DR2 are the rectifier diodes to be produced DC output voltage. In the circuit schematic, V_o is the output voltage, C_o is the output filter capacitor, R_o is the load resistance and V_{in} is the input voltage, TR is the high frequency transformer with n turns ratio.

The simulated dc voltage gain characteristic of LLC converter as function of normalized switching frequency, f_s/f_{r1}, and based on load variation from open-circuit to short-circuit is given in Figure 2. The boost mode is activated when converter operates below resonance frequency, f_{r1}, and the buck mode is activated above f_{r1}. The converter operates as load-independent and with unity gain at f_{r1}. At this point, converter delivers maximum power to the output where resonant inductor and resonant capacitor are tuned. Therefore this point is usually selected design optimization point for constant output voltage

applications. However, switching frequency optimization around f_{r1} is difficult for the EV battery charge applications requiring wide output voltage variation [10],[12].
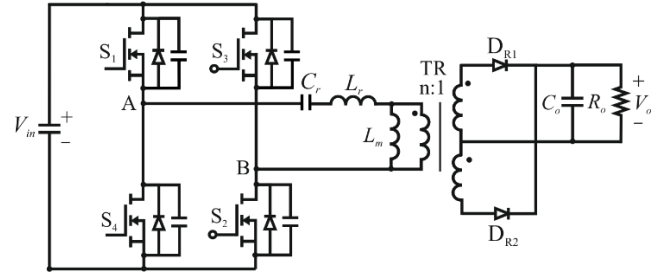

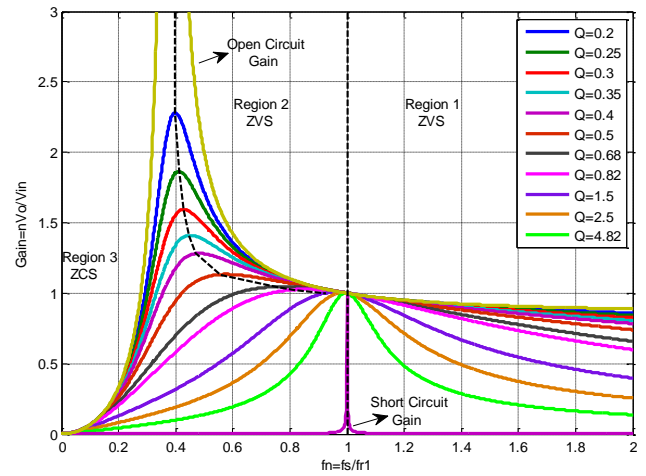Figure 1: The circuit schematic of LLC resonant converter for second stage of battery charger.

Figure 2: The typical dc voltage gain characteristics of LLC resonant converter as function of load and normalized switching frequency variation.

In the graphic given in Figure 2, f_{r1} is the first resonance frequency of LLC converter and it can be defined as;

$$f_{r1} = \frac{1}{2\pi\sqrt{L_r C_r}} \tag{1}$$

Where f_s is the switching frequency and the normalized switching frequency is defined as $f_n = f_s/f_{r1}$ The characteristic impedance of the resonant tank can be written as;

$$Z_o = \sqrt{\frac{L_r}{C_r}} \tag{2}$$

The quality factor is defined as follows:

$$Q = \frac{Z_o}{R_{ac}} \tag{3}$$

Where R_{ac} is the equivalent ac load resistance and it is defined as;

$$R_{ac} = \frac{8n^2}{\pi^2}\frac{V_o^2}{P_o} \tag{4}$$

Finally, the voltage gain of the converter based on FHA can be defined as;

$$Gain = \frac{nV_o}{V_{in}} = \frac{1}{1+\frac{L_r}{L_m}(1-\frac{f_{r1}^2}{f_s^2})+jQ(\frac{f_s}{f_{r1}}-\frac{f_{r1}}{f_s})} \quad (5)$$

As shown in the DC characteristic of LLC converter, zero voltage switching (ZVS) turn-on of primary MOSFETs can be achieved below and above f_{r1}. Therefore, for the wide output voltage range, converter can be operated in Region 1 and Region 2 to achieve high efficiency. In Region 1, series resonance between L_r nd C_r works and the input impedance of resonant tank is always inductive. Therefore, ZVS turn-on of the primary MOSFETS are under guarantee. However, soft commutations of rectifier diodes cannot be achieved for all load conditions, it is only possible under light load conditions [23],[12]. Moreover, the output voltage regulation under light load conditions is difficult.

Region 2 with inductive operation is the most preferred region for wide output voltage applications because soft switching operation of the primary MOSFETs and secondary rectifiers are provided for all load conditions. However, the borderline between inductive and capacitive region should be provided with optimum design to prevent the operation in capacitive region. In this region, two different operation mode occur and the operation of the converter is more complicated compared to Region 1. The equivalent circuits belong to operation intervals and the key waveforms are shown in Figure 3 and Figure 4, respectively.

As shown in Figure 3(a), at $t=t_0$, before the turn-on of S_1 and S_2 MOSFETs, their body diodes conduct to provide ZVS turn-on. The resonant current, i_{Lr}, increases as sinusoidal by the occurred series resonance between L_r and C_r. At the secondary side, D_{R1} diode conducts the output current and the magnetizing inductance is clamped by nV_o. Thus, magnetizing inductance doesn't attend the resonance in this stage and the current of magnetizing inductance increases linearly. As shown in Figure 3(b), at $t=t_1$, S_1 and S_2 MOSFETs are turned-on with ZVS and the current rise of L_r continues positively. At $t=t_2$, when the resonance current is equal to the magnetizing current, D_{R1} and D_{R2} diodes stay in off condition and the reflection of the output voltage to the primary side is removed as shown in Figure 3(c). Therefore, L_m attends the resonance between L_r and C_r. This operation stage ends when the S_1 and S_2 MOSFETs are turned-off under magnetizing current at $t=t_3$. At $t=t_3$, the resonant current starts to discharge the parasitic capacitor of S_3 and S_4 MOSFETs and charge the parasitic capacitors of S_1 and S_2 MOFETs as shown in Figure 3 (d). When the voltage of the parasitic capacitors reach to zero level at $t=t_4$, the antiparallel diode of S_3 and S_4 MOSFETs conduct. Thus, S_3 and S_4 can be turned-on with ZVS at $t=t_5$.

In Region 2, the conventional FHA method is not reliable to determine the borderline when switching frequency is far away from f_{r1} [12], [13]. In [24] and [25], steady state analysis is proposed to predict the behavior of LLC converter accurately but closed-form solution cannot be determined because of nonlinear and complex equations [13]. Therefore, switching frequency range, namely operation region, of LLC converter needs to be investigated for wide output voltage EV battery chargers.
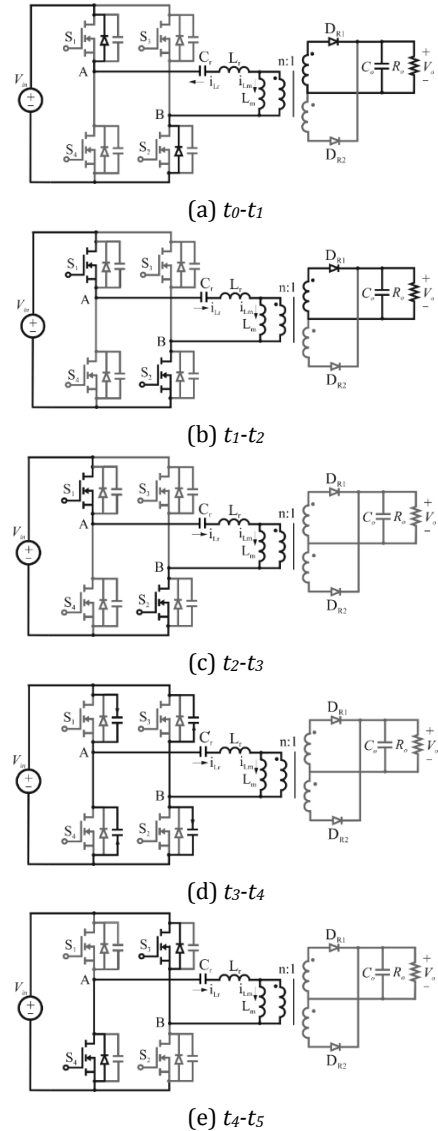

(a) t_0-t_1

(b) t_1-t_2

(c) t_2-t_3

(d) t_3-t_4

(e) t_4-t_5

Figure 3: Equivalent circuit belong to LLC converter for the operation below resonance. (a): t_0-t_1, (b): t_1-t_2, (c): t_2-t_3, (d): t_3-t_4. (e) t_4-t_5.
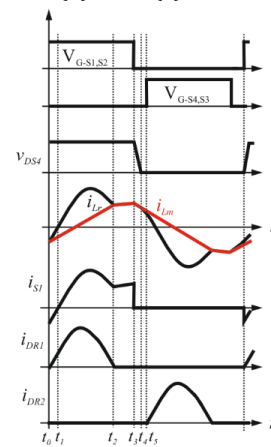

Figure 4: The key waveforms of LLC converter for the operation below resonance.

3 Design optimization

In this section, design optimization of the resonant tank components and power transformer of LLC converter is discussed to reach high efficiency and desired output voltage range. The resonant tank components, C_r, L_r and L_m, define the behavior of LLC converter. The optimization of the resonant tank parameters change depending on the output voltage range, switching frequency range and the power loss including switching and conduction loss.

Some initial parameters should be defined to start the optimization. The input voltage of the LLC converter is determined as 385 V. In the design procedure it is assumed that 14 li-ion battery cells are connected series in two parallel groups. Thus, 43.4-53.9 V / 30 A battery is assumed for the evaluation. The maximum power is determined as 1617 W. The resonant frequency, which gives maximum efficiency when converter is operated around it, is selected as 180 kHz. Design procedure of each component of LLC converter is given below.

3.1 Turns ratio of transformer

According to time weighted factor proposed in [13], 70% charge of a lithium-ion battery cell occurs in constant current mode while battery voltage is changes from 3.3 V to 3.5 V. Therefore, 3.4 V output voltage value can be determined at f_{r1} to reach high efficiency. For the 14 series lithium-ion battery cell, 48 V output voltage is selected at f_{r1} where the converter gain is unity. Thus, the turns ratio of the transformer can be determined as follows:

$$n = \frac{V_{in}}{V_o} \qquad (6)$$

3.2 Resonant inductor, L_r

The small values of the resonant inductor lead to high efficiency. However, there should be limit to prevent short circuit operation of the converter. The minimum resonant inductor can be selected to limit maximum output current in short circuit condition and limit the operation of the converter to its maximum switching frequency as given in [10]. According to this approach, L_r can be defined as follows:

$$L_{r-min} = \frac{V_{in}n}{8f_{s\,max}} \frac{V_{o-nom}}{P_o} \qquad (7)$$

Above, P_o is the output power, f_{smax} is the maximum switching frequency and V_{o-nom} is the nominal dc input voltage of the converter.

3.3 Resonant capacitor, C_r:

After determination of the resonant inductance, resonant capacitance can be obtained as follows:

$$C_r = \frac{1}{(2\pi f_o)^2 L_{r-min}} \qquad (8)$$

3.4 Magnetizing inductance, L_m

The magnetizing inductance controls the ZVS of the primary switches, turn-off current of the primary switches and the output voltage regulation. Therefore, it is the most important parameter in resonant tank and it should be designed properly.

The worst case for the ZVS of the primary switches is no load condition. Therefore, magnetizing inductance value can be determined taking into consideration the no load condition as follows:

$$L_{m-min} = \frac{nV_o t_{dead}}{4V_{in}(C_{S1}+C_{S4})f_s} \qquad (9)$$

Above equation is extracted for the charge and discharge of the parasitic capacitors of S_1 and S_4 MOSFETs, respectively. Therefore, C_{S1} and C_{S4} represent the parasitic capacitors of S_1 and S_4. Where t_{dead} is the dead time between the control signals of MOSFETs. The maximum current of L_m should be enough to discharge these capacitors, this condition can be defined as follows:

$$I_{m-peak} = \frac{nV_o T_s}{4L_m} \geq \frac{1}{2}(C_{S1}+C_{S4})V_{in}^2 \qquad (10)$$

As shown above equation, magnetizing inductance also control the turn-off current of the primary MOSFETs. To reduce turn-off current of the MOSFETs, magnetizing inductance can be selected large enough. However, very large magnetizing inductance design cannot provide the output voltage regulation since the magnetizing inductance also controls the output voltage regulation. If L_m is determined according to maximum output voltage as given in [10], [26], following statement can be written,

$$L_{m-max} = \frac{\pi^2}{4}L_r \frac{(1-\frac{f_{s-min}}{f_{r1}})}{(\frac{V_{in}}{nV_{o-max}}-1)} . \qquad (11)$$

Where, f_{s-min} is the minimum switching frequency to obtain maximum voltage gain and V_{o-max} represents the required maximum output voltage.

According to design optimization discussed above, resonant tank components are obtained to be L_r=25 µH, C_r=31 nF and L_m=75 µH.

3.5 Optimization of operation region and switching frequency range of LLC converter

In this section, three operation points of switching frequency which is above resonance, below resonance, and above-below resonance were evaluated by Saber simulation for high efficiency at wide output voltage range. The maximum and minimum output voltage of the converter are determined from the heavy load to the light load conditions. Table 1 summarizes the evaluation results performed for the different operation conditions.

For the operation below resonance, the converter works in Region 2. The output voltage is determined as 42 V near f_{r1} and then switching frequency is reduced to obtain higher output voltage range. Thus, turns ratio of the transformer is chosen as 9 to set 42 V at f_{r1}. However, targeted maximum output voltage is not obtained in Region 2 which provides soft switching operation for the primary switches and the secondary rectifiers. The decreasing switching frequency further puts the converter in Region 3 which is avoided. Therefore operation only below the f_{r1} is not suitable for targeted output voltage range of the converter as shown in the results given in Table 1.

In the operation above resonance, converter works in Region 1. The maximum output voltage is determined near f_{r1} and the switching frequency is increased to provide lower output

voltage range. Thus, turns ratio of the transformer is chosen as 7 to set 54 V at f_{r1}. As shown in Table 1, the required output voltage range is obtained at the frequency range changing from 80 kHz to 133.3 kHz.

In the operation above-below resonance, converter works in Region 1 and Region 2. According to time weight factor proposed in [13], 70% charge of the battery is completed around 3.4 V of battery voltage. Therefore, for series 14 li-ion battery, 48V output voltage value is chosen near f_{r1} point which provides maximum efficiency with reduced resonant tank impedance. At this point turns ratio of the transformer is determined as 8 to set 48 V at f_{r1}. Then the required switching frequency range is determined as 150 kHz-200 kHz for the targeted output voltage range as shown in Table 1.

Table 1: The output voltage and switching frequency range for different operation conditions.

Operation Condition	n	f_{r1}	f_s	V_0
$f_s \leq f_{r1}$	9	180 kHz	80-180 kHz	47-42 V
$f_s \geq f_{r1}$	7	80 kHz	80-133.3 kHz	54-42 V
$f_s \leq f_{r1} \& f_s \geq f_{r1}$	8	180 kHz	150-200 kHz	42-54 V

The output voltage range can be obtained with the operation above resonance and above-below resonance according to obtained results. Below resonance, in Region 2, a boundary preventing the operation in Region 3 should be provided to guarantee ZVS turn-on of the primary switches. The primary switches always turn-on with ZVS above resonance without any limitation. However soft commutation of the rectifier diodes appears just in light load conditions above resonance [23],[24] while they always operate with ZCS below resonance. Therefore, effects of the operation regions on efficiency should be investigated to determine the appropriate operation region of the converter.

The lithium-ion battery charge characteristic has two operation conditions which are constant current operation condition and constant voltage operation condition. Therefore, efficiency performance of the converter should be discussed based on that operation conditions. To simulate battery charge characteristic, a variable resistor can be used as the load of the converter.

An efficiency comparison for two operation mode is given in Figure 5. Comparison results are obtained by Saber simulation because FHA is not reliable when the switching frequency is far away from the f_{r1}. Figure 5(a) and Figure 5(b) shows the efficiency variations as function of the output voltage and output current, respectively. In the efficiency calculation, conduction and switching loss of the semiconductors, the conduction and the core loss of the magnetic components were taken into consideration. The turn-on switching loss of MOSFETs is almost zero and is not included the efficiency calculations. Some of the equations used in the calculations can be given as follows:

The conduction and turn-off switching loss of the MOSFET can be calculated with

$$P_{cond-MOS} = I_{RMS-MOS}{}^2 R_{DS-MOS} \tag{12}$$

$$P_{sw-off-MOS} = \frac{1}{2} I_{off-MOS} V_{in} t_f f_s \tag{13}$$

Where, I_{RMS} is the RMS current value flowing in MOSFET, R_{DS-MOS} is the on resistance of the MOSFET, $I_{off-MOS}$ is the turn-off current value of the MOSFET, t_f is the falling time of the MOSFET current.

The conduction loss of the secondary rectifier can be calculated with

$$P_{cond-rec} = \frac{I_o}{2} V_{FW-on} \tag{14}$$

Above, V_{FW-on} is the forward voltage drop of the diode. The conduction loss of the transformer can be calculated by

$$P_{cond-TR} = I_{RMS-pr}{}^2 R_{pr-AC} + 2 I_{RMS-sec}{}^2 R_{sec-AC} \tag{15}$$

The core loss was calculated based on Steinmetz equation and datasheet parameters of the core material. The power loss of the resonant inductor was calculated with the same principles applied for the transformer. Finally efficiency of the converter can be defined as;

$$\eta = \frac{P_o}{P_o + P_{sem} + P_{mag}} \tag{16}$$

P_o is the output power, P_{sem} is the total power loss of the semiconductors at the primary and secondary side, P_{mag} is the power loss of the magnetic components including power transformer and the resonant inductor.

According to calculation results given in Figure 5(a) and (b), the best efficiency is obtained for the operation of above-below resonance. The reduced turns ratio of the transformer above resonance operation results in decreased efficiency. However, during the constant current operation mode, the efficiency values closes each other during the regulation of lower values of the output voltage due to the increased switching frequency in above-below resonance operation.
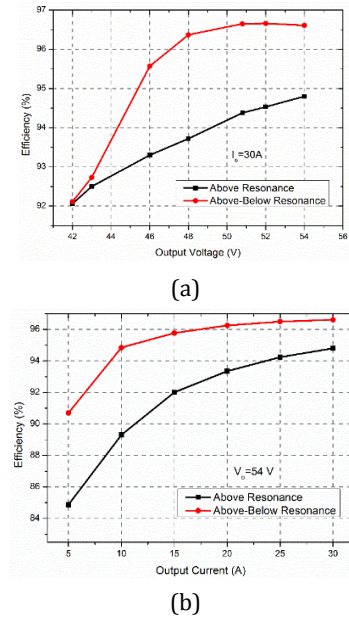

(a)

(b)

Figure 5: The efficiency calculations of LLC converter in the operation above resonance and above-below resonance. (a): Under full load condition with varying output voltage and, (b): Under varying load condition with maximum output voltage.

4 Simulation results

The operation of the proposed optimization procedure for the LLC resonant converter to be used in EV battery charge application is performed by Saber simulation. In the simulation, practical circuit components are modeled and operated to predict real operation conditions and results. The simulated circuit schematic is shown in Figure 6. 385 V nominal dc voltage is assumed for the input of the converter. The used semiconductors and magnetic components are summarized in Table 2. The operation of the LLC converter is evaluated for wide output voltage and load ranges taking into consideration the lithium-ion battery charge characteristic. For the operation above-below resonance, providing best efficiency, the converter was tested for the soft switching operation of primary MOSFETs and the output voltage regulation. Firstly, the converter is operated below resonance to obtain targeted maximum output voltage with full load condition. Figure 7 shows the obtained results for the maximum available output voltage. The obtained current and waveforms for the primary

switch, S_2, validate the ZVS turn-on process as shown in Figure 7(a). The rectifier diodes also softly commutate. The output voltage regulation under heavy load condition is achieved as shown in the Figure 7(b). The output voltage is obtained as 54.9 V and the average value of the rectified output current is 30.22 A at 150 kHz switching frequency.

Table 2: The used and modeled circuit components in Saber simulation.

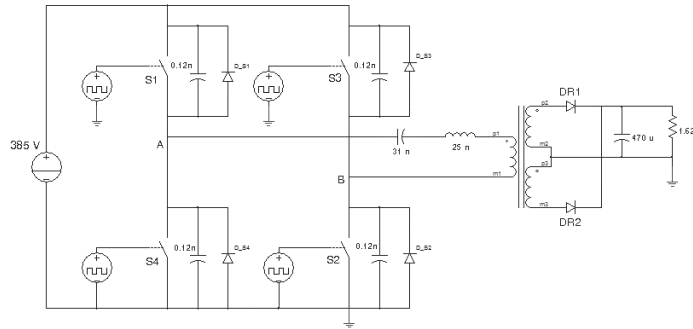| Parameters	Values
f_s	150-200 kHz
f_{r1}	180 kHz
S_1-S_4	SiC CMF20120D
D_{R1}-D_{R4}	DSSK 60-02A
TR	E/65/32/27, N_p=16, N_s=2
L_r	25 µH
C_r	31 nF
L_m	75 µH

Figure 6: The simulated circuit schematic of LLC resonant converter.
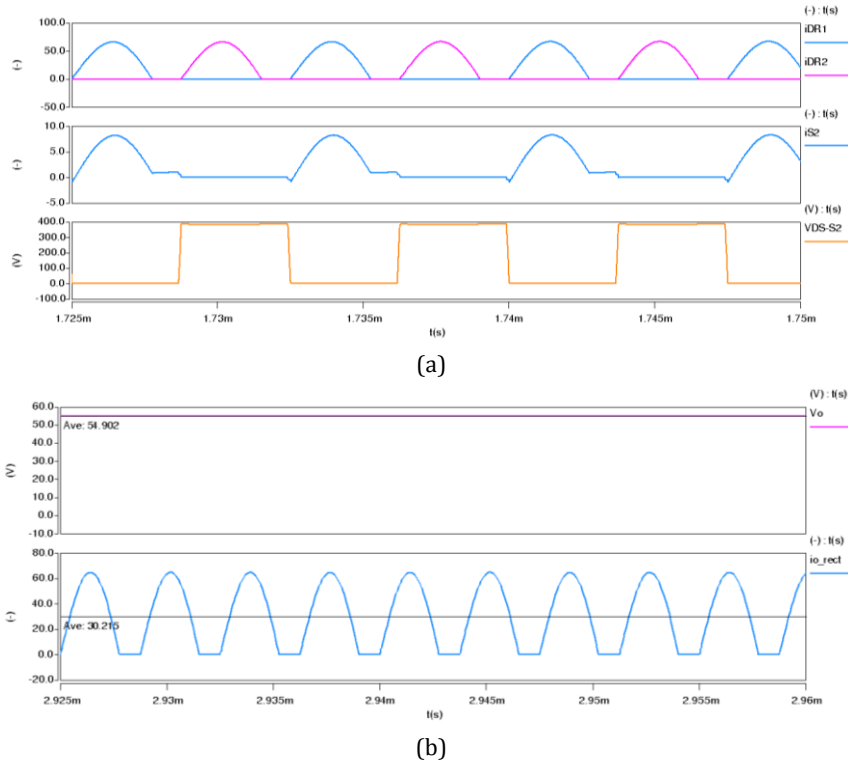

(a)

(b)

Figure 7: Simulated results below resonance for the maximum output voltage and full load condition. (a): Operation of the primary switches and rectifier diodes, (b): Regulated output voltage and rectified output current values.

Figure 8 shows the obtained results for the minimum output voltage with full load condition at 200 kHz operation frequency. The ZVS turn-on process of the primary switches are provided perfectly as shown in Figure 8 (a). However, soft commutation of the rectifier diodes are lost in this operation. The use of schottky diodes eliminate the reverse recovery losses. The output voltage and the average value of the rectified output current are obtained as 41.84 V and 29.99 A, respectively.

When the battery charged to the maximum output voltage, constant voltage mode operates and output current decreases. To evaluate the operation under light load conditions, the converter is operated for maximum output voltage with light load at 160 kHz operation frequency. The obtained results are given in Figure 9. The soft switching operation of the primary

switches and rectifier diodes are maintained. The maximum output voltage is determined as 55.2 V. The average value of the rectified output current is 4.92 A.

According to simulation results, the targeted output voltage range can be achieved at 150-200 kHz switching frequency range while soft switching operation of the primary switches is maintained.

In the operation of the converter, EMI (Electro Magnetic Interference) effects are not very important near 200 kHz due to soft switching operation of the converter. If serious EMI effects are observed in the practical application of the converter, a common mode filter can be adapted to the input of the converter.
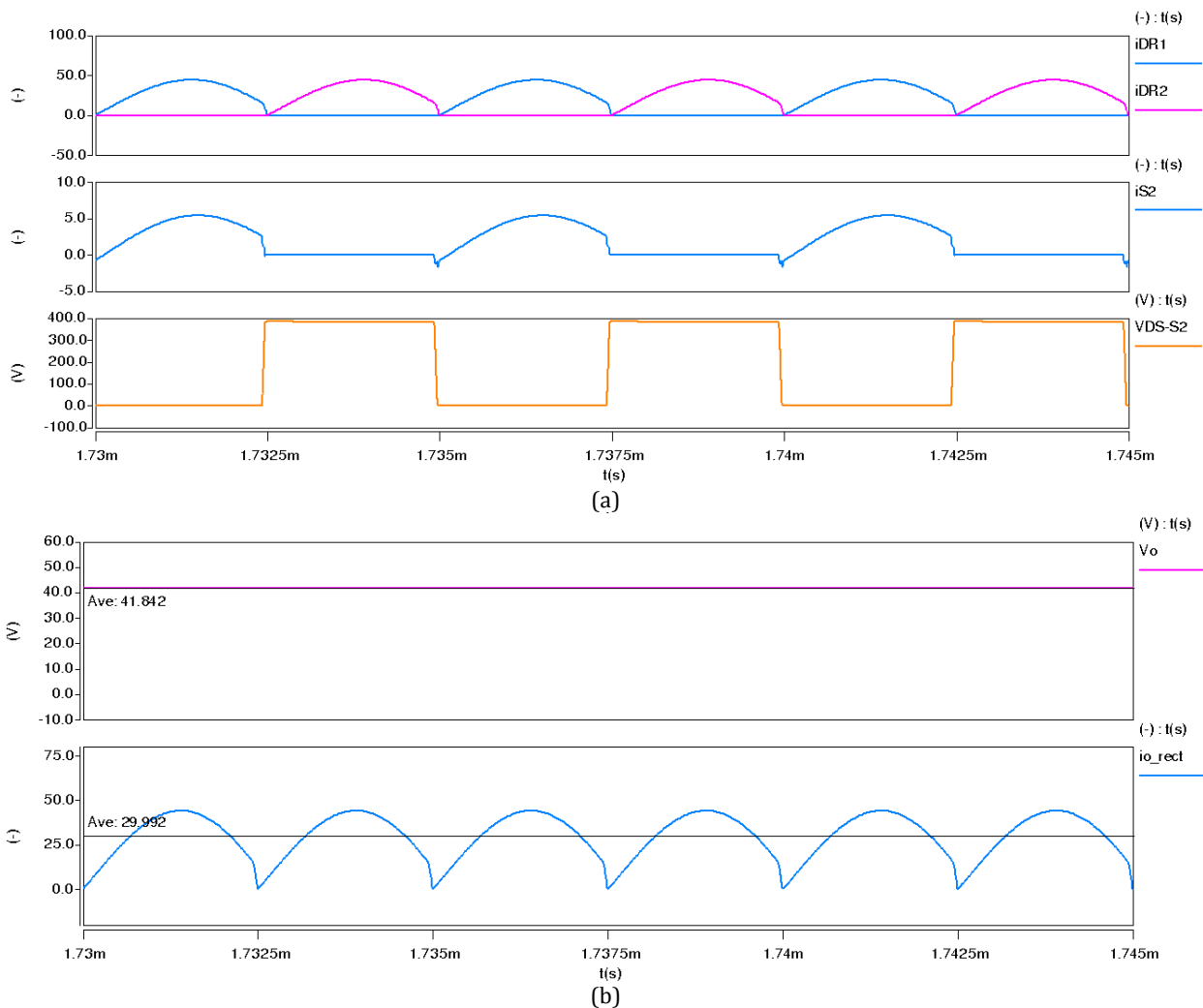

Figure 8: Simulated results for the operation of above resonance for the minimum output voltage and full load condition, (a): Operation of the primary switches and rectifier diodes, (b): Regulated output voltage and rectified output current values.
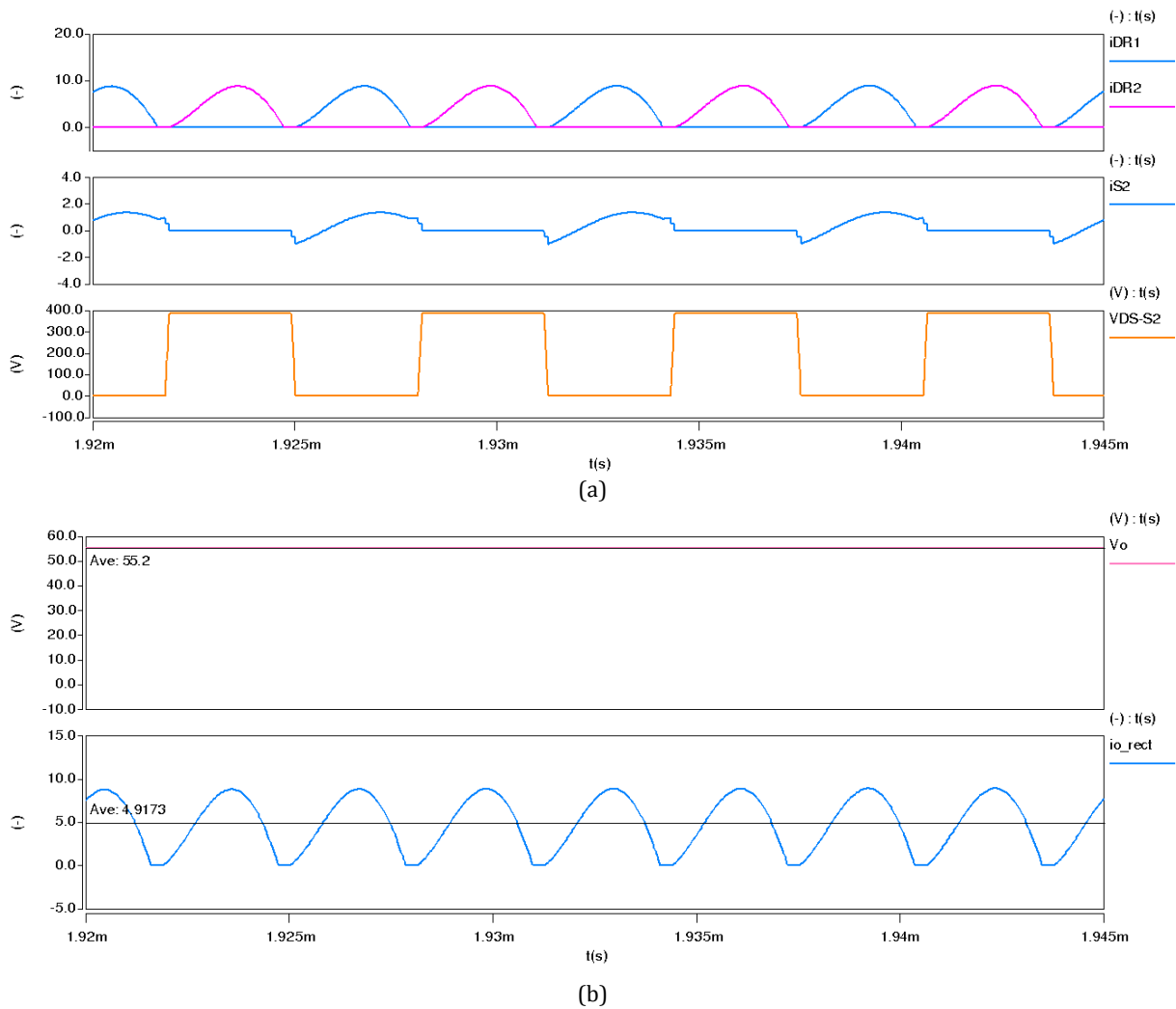
(a)

(b)

Figure 9: Simulated results for the operation of above resonance for the maximum output voltage and light load condition, (a): Operation of the primary switches and rectifier diodes, (b): Regulated output voltage and output current values.

5   Conclusions

In this study, the operation of a LLC converter is evaluated for EV battery charge applications. The operation region optimization based on high efficiency is evaluated to regulate wide output voltage range required in lithium-ion battery charge application. Because the conventional FHA method is not reliable when switching frequency is far away from the resonance frequency, Saber simulation model is used to optimize the operation region of LLC converter. Efficiency comparison graphics for different operations are extracted to determine the best operation region. Finally, according to optimized region, soft switching operation of LLC converter and the output voltage regulation are validated by simulation. 385 V DC voltage is applied to the input of LLC resonant converter. Then the targeted output voltage range from 42 V to 54V is obtained while soft switching operation of the primary MOSFETs is maintained. The maximum power of the converter is 1617 W. The maximum efficiency is determined as 96.6% with the presented design procedure.

6   References

[1]   Whitaker B, Barkley, A, Cole Z, Passmore B, Martin D, McNutt TY, Lostetter AB, Lee JS, Shiozaki K. "A high-density, high-efficiency, isolated on-board vehicle battery charger utilizing silicon carbide power devices". *IEEE Trasactions on Power Electronics*, 29(5), 2606-2617, 2014.

[2]   Yilmaz M, Krein PT. "Review of battery charger topologies, charging power levels and infrastructure for plug-in electric and hybrid vehicles". *IEEE Transactions on Power Electronics*, 28(5), 2151-2169, 2013.

[3]   Grenier M, Aghdam MH, Thiringer T. "Design of on-board charger for plug-in hybrid electric vehicle". *5. IET International Conference on Power Electronics, Machine and Drives*, Brighton, UK, 19-21 April 2010.

[4]   Haghbin S, Khan K, Lundmark S, Alak¨ula M, Carlson O, Leksell M, Wallmark O. "Integrated chargers for EV's and PHEV's: Examples and new solutions". *XIX International Conference on Electrical Machines*, Rome, Italy, 6-8 September 2010.

[5] Emadi A, Lee YJ, Rajashekara K. "Power electronics and motor drives in electric, hybrid electric and plug-in hybrid electric vehicles". *IEEE Transaction on Industrial Electronics*, 55(6), 2237-2245, 2008.

[6] Emadi A, Williamson SS, Khaligh A. "Power electronics intensive solutions for advanced electric, hybrid electric and fuel cell vehicular power systems". *IEEE Transactions on Power Electronics*, 21(3), 567-577, 2006.

[7] Gautam DS, Musavi F, Edington M, Eberle W, Dunford WG. "An automotive onboard 3.3-kW battery charger for PHEV application". *IEEE Transsctions on Vehicular Technology*, 61(8), 3466-3474, 2012.

[8] Chen M, Rinc´on-Mora GA. "Accurate, compact and power-efficient li-ion battery charger circuit". *IEEE Transactions on Circuits and Systems-II: Express Briefs*, 53(11), 1180-1184, 2006.

[9] Dearborn S. "Charging li-ion batteries for maximum run times". *Power Electronics Technology*, 31(4), 40-49, 2005.

[10] Musavi F, Craciun M, Gautam DS, Eberle W, Dunford WG. "An LLC resonant DC-DC converter for wide output voltage range battery charging applications". *IEEE Transactions on Power Electronics*, 28(12), 5437-5445, 2013.

[11] Sun W, Wu H, Hu H, Xing Y. "Resonant tank design considerations and implementation of a LLC resonant converter with a wide battery voltage range". *Journal of Power Electronics*, 15(6), 1446-1455, 2015.

[12] Deng J, Li S, Hu S, Mi CC, Ma R. "Design methodology of LLC resonant converters for electric vehicle battery chargers". *IEEE Transactions on Vehicular Technology*, 63(4), 1581-1592, 2014.

[13] Fang Z, Cai T, Duan S, Chen C. "Optimal design methodology for LLC resonant converter in battery charging applications based on time-weighted average efficiency". *IEEE Transactions on Power Electronics*, 30(10), 5469-5483, 2015.

[14] Kim JW, Kim DY, Kim CE, Moon GW. "A simple switching control technique for improving light load efficiency in a phase-shifted full-bridge converter with a server power system". *IEEE Transactions on Power Electronics*, 29(4), 1562-1566, 2014.

[15] Kim DY, Kim CE, and Moon GW. "Variable delay time method in the phase-shifted full-bridge converter for reduced power consumption under light load conditions". *IEEE Transactions on Power Electronics*, 28(11), 5120-5127, 2013.

[16] Steigerwald LR. "A comparison of half-bridge resonant converter topologies". *IEEE Transactions on Power Electronics*, 3(2), 174-182, 1988.

[17] Lu B, Liu W, Liang Y, Lee FC, Van Wyk JD. "Optimal design methodology for LLC resonant converter". *Twenty-First Annual IEEE Applied Power Electronics Conference and Exposition APEC '06*, Blacksburg, USA, 19-23 March 2006.

[18] Fang Y, Xu D, Zhang Y, Gao F, Zhu L. "Design of high power density LLC resonant converter with extra wide input range". *Twenty-Second Annual IEE Applied Power Electronics Conference*, Anaheim, USA, 25 February-1 March 2007.

[19] Huang D, Gilham D, Feng W, Kong P, Fu D, Lee FC. "High power density high efficiency DC-DC converter". *Energy Conversion Congress and Exposition (ECCE)*, Phoenix, USA, 17-22 September 2011.

[20] Biela J, Badstuebner U, and Kolar JW. "Design of a 5-kW, 1-U, 10-kW/dm³ resonant DC-DC converter for telecom applications". *IEEE Transactions on Power Electronics*, 24(7), 1701-1710, 2009.

[21] Dow YS, Son HI, Lee HD. "A study on half bridge LLC resonant converter for battery charger on board". *8th International Conference on Power Electronics-ECCE Asia*, Jeju, Island, 30 May-3 June 2011.

[22] Dow YS, Kim HH, Kwon YI, Kim BY, Kim JC. "A study of 6.6 kW on board charger for electric vehicle". *EVS28 International Electric Vehicle Symposium and Exhibition*, Kintex, Korea, 3-6 May 2015.

[23] Fang X, Hu H, Shen ZJ, Batarseh I. "Operation mode analysis and peak gain approximation of the LLC resonant converter". *IEEE Transactions on Power Electronics*, 27(4), 1985-1995, 2012.

[24] Lazar JF and Martinelli R. "Steady-State analysis of the LLC series resonant converter". *16th Annual IEEE Applied Power Electronics Conference and Exposition*, Anaheim, USA, 4-8 March 2001.

[25] Yu R, Ho GKY, Pong BMH, Ling BWK, Lam J. "Computer aided design and optimization of high efficiency LLC series resonant converter". *IEEE Transactions on Power Electronics*, 27(7), 3243-3256, 2012.

[26] Gu Y, Lu Z, Hang L, Qian Z, Huang G. "Three-Level LLC series resonant DC/DC converter". *IEEE Transactions on Power Electronics*, 20(4), 781-789, 2005.